

Valence spin observables in hard-scattering QCD and the measurement of the gluon spin density

Gordon Ramsey

Physics Department, Loyola University Chicago, Chicago, Illinois 60626

Dennis Sivers

High Energy Physics Division, Argonne National Laboratory, Argonne, Illinois 60439

(Received 17 September 1990)

To test the validity of the QCD-based hard-scattering model for spin-dependent measurements, it is useful to define observables which depend only on the valence-quark spin distributions. If theory proves an effective guide to these "valence" observables, the valence-quark contribution to other spin-dependent large- p_T processes can be specified with similar accuracy. We can then formulate large- p_T measurements which determine the gluon spin density in a polarized proton.

I. INTRODUCTION

Results from the European Muon Collaboration (EMC) experiment¹ continue to focus interest on the question of the spin content of the proton. Comparing the data to the Ellis-Jaffe² sum rule, one obtains the surprising inference that the net spin carried by the quarks and antiquarks comprises only a small fraction of the total proton spin.³⁻⁵ Since the EMC data were first presented, a number of diverse models have been devised to explain this observation.⁶⁻⁸ Because of the diversity of theoretical opinion it is now important to clarify the question of the proton spin composition experimentally.

The extraction of the necessary spin information requires a broadly based experimental program. As a first step, remeasurement of $g_1^p(x, Q^2)$ in deep-inelastic lepton scattering along with the measurement of $g_1^n(x, Q^2)$ will allow an experimental test of the Bjorken sum rule.⁹ However, in order to address directly the question of the gluon polarization density it is necessary to go beyond deep-inelastic lepton scattering. The determination of the spin-weighted gluon density $\Delta G(x, Q^2)$ necessarily involves the measurements of such two-spin asymmetries as $a_{LL} d\sigma(pp \rightarrow \pi X)$, $a_{LL} d\sigma(pp \rightarrow \text{jet}, X)$,¹⁰ or $a_{LL} d\sigma(pp \rightarrow \gamma X)$ ¹¹ for large transverse-momentum production with polarized proton beams and targets. The asymmetry a_{LL} is defined to be the cross section for initial helicities the same minus the cross section for helicities opposite divided by the sum of the two cross sections, i.e.,

$$a_{LL} \equiv \frac{\sigma(\rightarrow\rightarrow) - \sigma(\rightarrow\leftarrow)}{\sigma(\rightarrow\rightarrow) + \sigma(\rightarrow\leftarrow)}.$$

Its use as a probe of hard-scattering dynamics is discussed in Ref. 10.

These high- p_T production experiments raise a set of theoretical questions of their own. The use of perturbative QCD in the context of a hard-scattering model has made possible a number of important predictions. However, because of large correction factors in the formulation of the QCD-based parton model, it is hard to specify

the validity of the model at any given value p_T .¹² As an example of this uncertainty, we note that there remains a large ambiguity the determination of the unpolarized gluon distribution,¹³ in spite of a large amount of data. These limitations are very important in the analysis of polarized-beam experiments. Because the luminosity of polarized beams is low compared to that of unpolarized beams, experimental constraints dictate that asymmetry measurements will not be available over the maximum range of kinematic variables in which the spin-averaged inclusive cross sections can be measured.

In order to determine the gluon spin density $\Delta G(x, Q^2)$ with sufficient accuracy to discriminate between models of proton structure, it is important to have assurance that the spin-dependent data are free from possible nonfactorizing, higher-twist corrections which would distort the theoretical interpretation. We believe that the best way to obtain the necessary confidence in the underlying theoretical formalism is to form flavor-nonsinglet quantities from the experimental data. These quantities can be calculated in hard-scattering QCD from *valence*-quark spin distributions which are comparatively well determined from the deep-inelastic lepton scattering experiments. Comparison of theoretical predictions with experimental data can therefore be used to validate or to rule out the use of the QCD hard-scattering model within a given kinematic regime.

Two examples of the type of nonsinglet observables which can provide the desired calibration are

$$A_{LL}^{\text{DV}}(\pi^0) = \frac{a_{LL} d\sigma(p\bar{p} \rightarrow \pi^0 X) - a_{LL} d\sigma(pp \rightarrow \pi^0 X)}{d\sigma(p\bar{p} \rightarrow \pi^0 X) - d\sigma(pp \rightarrow \pi^0 X)}, \quad (1.1a)$$

and

$$A_{LL}^{\text{DV}}(\gamma) = \frac{a_{LL} d\sigma(p\bar{p} \rightarrow \gamma X) - a_{LL} d\sigma(pp \rightarrow \gamma X)}{d\sigma(p\bar{p} \rightarrow \gamma X) - d\sigma(pp \rightarrow \gamma X)}. \quad (1.1b)$$

In this paper, we will give predictions for these ratios based on the valence-quark spin densities extracted from our analysis¹⁴ of the deep-inelastic lepton scattering data. When data from forthcoming experiments using polar-

ized beams are compared with these calculations, we can expect that uncalculable spin-dependent forces will give higher-twist effects which will cloud the comparison at low values of p_T but that the agreement will improve as p_T and \sqrt{s} are increased. We hope that at some point there will exist a range of p_T for which the hard-scattering QCD parton model is providing a quantitative description of the data. This will then define the value of transverse momentum for which spin observables involving other parton densities become interesting. We have no way of specifying *a priori* when this will occur but one can hope that experiments now underway with polarized p and \bar{p} beams will have some impact on the issue.

When there exists a region of p_T and \sqrt{s} where the hard-scattering QCD formalism is known to be a valid approximation to $A_{LL}^{DV}(\pi^0)$ or $A_{LL}^{DV}(\gamma)$, it also becomes possible to estimate the valence-quark contribution to a large number of other two-spin asymmetries and to separate processes involving gluons. Therefore, it is possible to determine the sensitivity of a particular measurement to the polarization of the gluons. We describe this process for the observable $a_{LL}(pp \rightarrow \pi^0 X)$. In doing this exercise, we find that $a_{LL}(pp \rightarrow \pi^0 X)$ should be very large if the gluons in a proton are fully polarized with $\Delta G(x, p_T^2)/G(x, p_T^2) \cong 1$ for $x \geq 0.04$ as is suggested by some recent theoretical speculation.^{15,16} Therefore, if upcoming experiments support the QCD hard-scattering prediction for $A_{LL}^{DV}(\pi^0)$, they may also be able to confirm or to rule out these speculative suggestions concerning the gluonic spin component.

A more stringent test is to see whether data on this process can be used to distinguish the possibilities $\Delta G(x, p_T^2)/G(x, p_T^2) \cong x$ and $\Delta G(x, p_T^2)/G(x, p_T^2) \cong 0$. We will see that potential experimental errors for the various components in the puzzle would have to be quite small in order to have a measurement of the gluon spin density at this level of accuracy. Without significant improvement in experimental techniques (such as the storage of polarized proton beams in colliders) we believe it will prove difficult to obtain a measurement of $\Delta G(x, p_T^2)$ which will confront traditional ideas of hadron structure.

In this paper we will also discuss calculations for the quantity $\Delta\sigma_L^{\text{jet}}(\sqrt{s}, p_0)$.¹⁷ This observable has previously been shown to be sensitive to the existence of strongly polarized gluons.¹⁸ The jet cross section provides a good starting point for the consideration of uncertainties associated with higher-order perturbative corrections and with the existence of possible higher-twist dynamics.

We begin our efforts with a discussion in Sec. II of the spin-weighted parton distributions. This section serves to fix our definitions and introduces some of the conventions used to discuss the "valence" asymmetries given in Sec. III. Section III is almost self-contained and can be considered independently of our models. Section IV gives some specific calculations which serve to demonstrate our basic points.

II. PARTON SPIN DENSITIES

The application of factorization theorems in perturbative QCD (Ref. 19) assures that it is possible to determine

a set of parton distributions by measuring some basic processes and then to use these distributions in calculations which predict a large number of other observables. Although there are a number of qualifications which prudence suggests should remain attached, a claim of success for the structure of the QCD parton model now seems warranted. We note here that the parton-model factorization can be carried out for hadrons in a definite longitudinal spin state. Using the spin-dependent properties of the constituent hard-scattering processes calculated in perturbation theory,¹⁰ it is possible to take measurements of spin-weighted parton densities and make predictions for various two-spin asymmetries.

However, any such predictions are limited by the processes in which the spin-dependent parton distributions are measured. In analogy to spin-averaged quantities, the natural place to determine the quark distributions is in the deep-inelastic scattering of a polarized lepton with a polarized hadron target. We will not dwell here on the analysis of deep-inelastic muon scattering experiments but will summarize the determination of the parton densities found in our work in Ref. 14. We define process-independent parton distributions which obey lowest-order Altarelli-Parisi equations. For the up and down quarks we distinguish between valence and sea components

$$\begin{aligned} u(x, Q^2) &= u_v(x, Q^2) + u_s(x, Q^2), \\ d(x, Q^2) &= d_v(x, Q^2) + d_s(x, Q^2). \end{aligned} \quad (2.1)$$

For each flavor ($i = u_v, d_v, u_s, d_s, \bar{u}, \bar{d}, s, \bar{s}, \dots$) of quark we have the spin-weighted difference

$$\Delta q^i(x, Q^2) = q_{+/+}^i(x, Q^2) - q_{-/+}^i(x, Q^2), \quad (2.2)$$

where the plus and minus refer to the Z component of quark and proton spin, respectively. This density appears in the calculation of spin-weighted observables for various hard-scattering processes.

Following Carlitz and Kaur²⁰ and Ref. (14) we will parametrize the polarization of the valence quark distributions in the form

$$\begin{aligned} \Delta u_v(x, Q^2) &= \cos\theta_D(x, Q^2)[u_v(x, Q^2) - \frac{2}{3}d_v(x, Q^2)], \\ \Delta d_v(x, Q^2) &= -\frac{1}{3}\cos\theta_D(x, Q^2)d_v(x, Q^2), \end{aligned} \quad (2.3)$$

where θ_D is a valence quark-spin-dilution angle which measures the deviation of the spin-weighted distributions from the SU(6) limit. Measurements in deep-inelastic scattering indicate that

$$\lim_{x \rightarrow 1} \cos\theta_D(x, Q^2) = 1. \quad (2.4)$$

Just as measurements of spin-averaged deep-inelastic scattering enable us to extract reasonably stable estimates of $u_v(x, Q^2)$ and $d_v(x, Q^2)$, the longitudinal asymmetry A_1 measured in lepton scattering allows us to determine $\Delta u_v(x, Q^2)$ and $\Delta d_v(x, Q^2)$ with an uncertainty compara-

ble to the underlying experimental error. The model of Ref. 14 gives the spin-weighted distributions, $\Delta u_v(x, Q^2)$ and $\Delta d_v(x, Q^2)$ and the unpolarized valence quark distributions $u_v(x, Q^2)$ and $d_v(x, Q^2)$ shown in Fig. 1. Although the uncertainties in the determination of these spin-weighted distributions are large compared to those on the spin-averaged valence distributions, they are tractable in that they provide testable predictions for other two-spin asymmetries. The nature of these uncertainties will be discussed in Sec. IV in terms of our model fits to the deep-inelastic data.

By way of contrast, we have absolutely no information on the spin-weighted gluon distribution

$$\Delta G(x, Q^2) = G_{+/+}(x, Q^2) - G_{-/+}(x, Q^2) \quad (2.5)$$

for gluons in a spin- $\frac{1}{2}$ proton. We can parametrize the three possible spin projections of the gluon along the z axis in terms of two angles Φ_L and θ_g , whereby

$$\begin{aligned} G_{+/+}(x, Q^2) &= \left[\left(\frac{1 + \cos\Phi_L}{2} \right)^2 \cos^2\theta_g \right. \\ &\quad \left. + \left(\frac{1 - \cos\Phi_L}{2} \right)^2 \sin^2\theta_g \right] G(x, Q^2), \\ G_{0/+}(x, Q^2) &= \frac{1}{2} \sin^2\Phi_L G(x, Q^2), \\ G_{-/+}(x, Q^2) &= \left[\left(\frac{1 + \cos\Phi_L}{2} \right)^2 \sin^2\theta_g \right. \\ &\quad \left. + \left(\frac{1 - \cos\Phi_L}{2} \right)^2 \cos^2\theta_g \right] G(x, Q^2). \end{aligned} \quad (2.6)$$

For ‘‘on-shell’’ gluons with no transverse momentum, $\Phi_L = 0$ and the scalar polarization density $G_{0/+}(x, Q^2)$ vanishes. Polarized gluons contribute to the spin of the

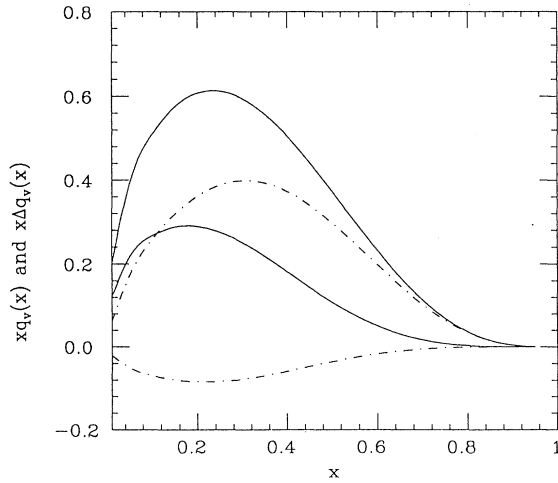


FIG. 1. The unpolarized valence-quark distributions $xu_v(x)$ (upper solid curve) and $xd_v(x)$ (lower solid curve) and the polarized valence quark distributions $x\Delta u_v(x)$ (upper dashed curve) and $x\Delta d_v(x)$ (lower dashed curve), as a function of x at $Q^2 \cong 10.7 \text{ GeV}^2$.

proton but the spin-weighted distribution $\Delta G(x, Q^2)$ in (2.5) is not measured directly by deep-inelastic lepton scattering asymmetries. In Sec. IV, we will return to the discussion of those processes in which, in principle, it can be determined.

Much of the interest in the gluon distribution (2.5) has been generated by some theoretical speculation. Altarelli and Ross¹⁵ as well as Carlitz, Collins, and Mueller¹⁶ have formulated an indirect argument for a large polarization of the gluons. The argument parallels the treatment of chiral symmetry in current algebra. Recasting the flavor-singlet axial-vector current in the form

$$\begin{aligned} J_\mu^5 &= J_\mu^c + n_f K_\mu, \\ K_\mu &= \frac{\alpha_s}{2\pi} \epsilon_{\mu\nu\rho\sigma} A_a^\nu (\partial^\rho A_a^\sigma - \frac{1}{3} g f_{abc} A_b^\rho A_c^\sigma), \end{aligned} \quad (2.7)$$

where n_f is the number of flavors, we recall that the current J_μ^c is conserved in the chiral limit when quark masses vanish. The divergence of the physical current, J_μ^5 is entirely associated with the ‘‘anomalous’’ gluonic contribution. The separation in (2.7) is not gauge invariant but many matrix elements are well defined and the split-up provides important insight.²¹

For the quarks and antiquarks in the sea, we can envision a similar split-up of the spin-weighted distributions

$$\begin{aligned} \Delta q_5^s(x, Q^2) &= \Delta q_c^s(x, Q^2) - \frac{\alpha_s(Q^2)}{4\pi} \hat{\gamma}(x) \otimes \Delta G(x, Q^2), \\ \Delta \bar{q}_5(x, Q^2) &= \Delta \bar{q}_c(x, Q^2) - \frac{\alpha_s(Q^2)}{4\pi} \hat{\gamma}(x) \otimes \Delta G(x, Q^2), \end{aligned} \quad (2.8)$$

where \otimes denotes convolution, $\hat{\gamma}(x)$ is convention dependent, and a renormalization prescription for $\alpha_s(Q^2)$ must be specified. The chiral distributions $\Delta q_c^s(x, Q^2)$ and $\Delta \bar{q}_c(x, Q^2)$ are chosen to obey the lowest-order Altarelli-Parisi equations²² so that their first moments do not evolve with Q^2 in the chiral limit, i.e.,

$$\begin{aligned} \frac{\partial}{\partial \ln Q^2} \langle \Delta q_c^s \rangle &= 0, \\ \langle \Delta q_c^s \rangle &\equiv \int_0^1 dx \Delta q_c^s(x, Q^2), \end{aligned} \quad (2.9)$$

while $\Delta q_5^s(x, Q^2)$ and $\Delta \bar{q}_5(x, Q^2)$ are defined in a deep-inelastic-scattering (DIS) scheme. At next-to-leading order in perturbation theory, the Q^2 evolution of the first moment of $\Delta q_5^s(x, Q^2)$ can therefore be identified with the Q^2 evolution of the quantity¹⁴

$$\Gamma(Q^2) = + \frac{\alpha_s(Q^2)}{4\pi} \langle \Delta G(Q^2) \rangle. \quad (2.10)$$

In this framework, a large negative polarization of the sea quarks and antiquarks as suggested by the EMC data can perhaps be reconciled with the nonrelativistic quark model and a small, unpolarized sea for the proton at small Q^2 by allowing for significant Q^2 dependence of $\Gamma(Q^2)$ between $Q^2 \cong m_p^2$ and $Q^2 \cong 10 \text{ GeV}^2$ (the average value of Q^2 in the EMC experiment).

In focusing on the anomaly, this argument neglects other, nonperturbative, dynamics^{4,14} which can lead to

the negative polarization of the sea. Taken at face value and combined with the EMC data the argument can lead to a surprisingly large amount of spin,

$$\langle \Delta G \rangle |_{Q^2 \approx 10} \approx 5-6, \quad (2.11)$$

associated with the gluons in a polarized proton. This large value is somewhat counterintuitive but since it is already known^{10,23,24} that perturbative QCD implies

$$\lim_{Q^2 \rightarrow \infty} \langle \Delta G \rangle = \infty, \quad (2.12)$$

it is not outside the realm of possibility.

These complex arguments have certain problems. For example, Bodwin and Qiu²⁵ have shown that the regulators used in Refs. 15 and 16 to make separation in (2.8) have problems either with gauge invariance or analyticity. To first order in α_s , a satisfactory regulator will give a vanishing contribution to the first moment of g_1^p from polarized gluons. Hence, the split-up in (2.8) is justified only by the presumed flavor dependence of the quantities involved rather than by a well-defined factorization procedure. Jaffe and Manohar²⁶ have expressed similar reservations phrased in the language of the operator-product expansion and at this time the suggestion that the EMC data lead to (2.11) remains highly speculative.

We do not intend to comment further at this point on the theoretical issues except to note that their thrust is to suggest (rather than compel) a possible strong polarization of the gluons. This possibility is worthy of consideration in the context of an experimental program to measure spin-dependent observables. Certain of these observables are sensitive to the gluon polarization. Included among these are the spin-weighted cross sections in jet production¹⁰ and the asymmetries in π or γ production¹¹ from pp and $p\bar{p}$ scattering.

For purposes of testing the spin-weighted distributions based on a QCD-aided parton model, we have constructed three models of the polarized glue. These represent extreme situations, ranging from no polarization to a maximum polarization suggested by the theoretical arguments mentioned above. The three parametrizations are

$$\begin{aligned} (1) \text{ no polarization: } \Delta G/G &= 0, \\ (2) \text{ small polarization: } \Delta G/G &= x, \\ (3) \text{ large polarization: } \Delta G/G &\begin{cases} 12.5x, & x \leq 0.08, \\ 1, & x > 0.08. \end{cases} \end{aligned} \quad (2.13)$$

The second model in (2.13) above is suggested by conventional Regge arguments which give $\Delta G/G \approx x^{\alpha_p - \alpha_A}$. The form of the third model was chosen so that $\int_0^1 dx \Delta G(x) \equiv \langle \Delta G(x) \rangle = 5.0$, an order of magnitude larger than the second parametrization. This third model is characteristic of those gluon distributions which have been considered in the post-EMC era to estimate two-spin asymmetries.²⁷ These models are shown as a function of x in Fig. 2. The Q^2 evolution for different forms of ΔG can be found in Ref. 14.

The spin-spin asymmetries we will discuss are not very sensitive to sea distributions. In Ref. 14 we gave two pa-

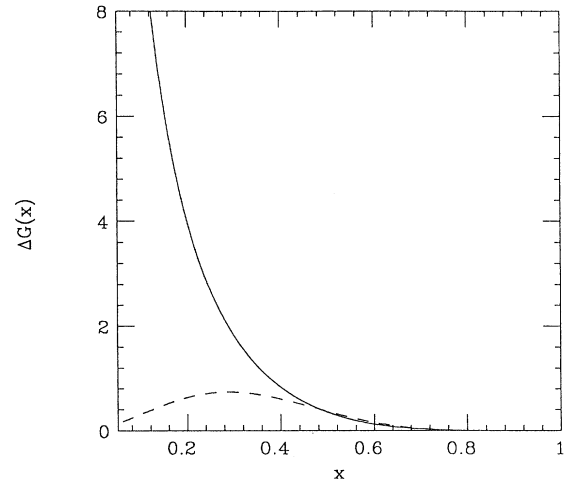


FIG. 2. The polarized gluon distribution models as a function of x . The dashed curve represents the small gluon polarization [Eq. (2.13), No. (2)] while the solid curve shows the large gluon polarization [Eq. (2.13), No. (3)].

rametrizations of the polarized sea distributions which represent a considerable range in the sea contribution to the spin of the proton. The polarized sea, however, does have an implicit bearing on the interpretation of the valence-quark polarization. For unpolarized distributions, the familiar assumption that the sea is even under charge conjugation gives

$$u_s(x, Q^2) = \bar{u}(x, Q^2). \quad (2.14)$$

However, because the spin-spin forces are not even under charge conjugation, there is generally no analogous relation for the spin-weighted distributions. In fact, specific models of two-body spin-dependent forces such as those examined in Ref. 14 suggest that the antiquarks may be more strongly polarized than the sea quarks. In general, we expect that

$$c |\Delta u_s(x, Q^2)| \cong |\Delta \bar{u}(x, Q^2)|, \quad (2.15)$$

with $c \geq 1$ and the relative magnitude of the two will affect the interpretation of the valence-quark contribution to the proton spin. We can define a charge-conjugation-odd form of the polarized valence-quark distribution in the usual way by subtraction:

$$\Delta u_{\text{val}}(x, Q^2) = \Delta u(x, Q^2) - \Delta \bar{u}(x, Q^2). \quad (2.16)$$

This will differ from the parametrization of Eq. (2.3),

$$\Delta u_v(x, Q^2) = \cos \Theta_D [u_v(x, Q^2) - \frac{2}{3} d_v(x, Q^2)], \quad (2.17)$$

which has no particular charge-conjugation symmetry by

a small amount. Since the $\Delta u(x, Q^2)$, in Eq. (2.16) contains both the valence and sea contributions, the particular model used to define the relative size of the polarized sea quarks to the polarized sea antiquarks will necessarily affect the definition of Δu_{val} . As the parametrization of Δu_v in Eq. (2.17) is fixed by the Bjorken sum rule, the distinction between Δu_{val} and Δu_v depends on the model of the polarized sea which is used to calculate the spin observables. In Sec. III, we will form charge-conjugation-odd valence quantities by taking differences of quantities measured in proton beams and antiproton beams, thus using Δu_{val} . In Sec. IV, where appropriate, we will plot the spin observables using two models of the sea polarizations to illustrate the range of interpretation of the valence-quark contributions to these quantities.

III. VALENCE QUANTITIES IN SPIN-DEPENDENT LARGE-TRANSFER-MOMENTUM PRODUCTION

In order to focus on the dynamics of the QCD hard-scattering model, it is often convenient to form flavor-nonsinglet quantities in which the contribution of many constituent subprocesses cancel out. An example of such a quantity is

$$\frac{E d\sigma}{d^3p}(p\bar{p} \rightarrow \pi^0 x) - \frac{E d\sigma}{d^3p}(pp \rightarrow \pi^0 x) \equiv \frac{E\sigma^{\text{DV}}}{d^3p}(\pi^0), \quad (3.1)$$

where the production of the π^0 is at large transverse momentum. For the spin-averaged pp process, we can write

$$\frac{E d\sigma}{d^3p}(pp \rightarrow \pi^0 x) = \frac{1}{\pi} \sum_{ab \rightarrow cd} \int dx_a dx_b G_{a/p}(x_a, \mu^2) G_{b/p}(x_b, \mu^2) \frac{1}{z_c} D_{\pi^0/c}(z_c, \mu^2) \left[\frac{d\hat{\sigma}}{d\hat{t}}(ab \rightarrow cd; \hat{s}, \hat{t}) \right], \quad (3.2)$$

where the sum over all subprocesses is indicated. When we take the difference between $p\bar{p}$ and pp initial states, all subprocesses involving initial sea quarks or gluons cancel. In addition, since in lowest-order perturbation theory we observe

$$\frac{d\sigma}{dt}(ud \rightarrow ud) = \frac{d\sigma}{dt}(u\bar{d} \rightarrow u\bar{d}), \quad (3.3)$$

these processes also cancel in the difference. Using isospin invariance we have equality among the different decay distributions

$$D_{\pi^0/u}(z, \mu^2) = D_{\pi^0/\bar{d}}(z, \mu^2) = D_{\pi^0/d}(z, \mu^2) = D_{\pi^0/\bar{u}}(z, \mu^2) \quad (3.4)$$

so that we can combine up and down contributions. (We will neglect the contributions of heavy quarks.) The ‘‘annihilation’’ cross section into final-state quarks can be defined as

$$\frac{d\sigma^{\text{ah}}}{dt}(s, t) \equiv \left[\frac{d\sigma}{dt}(u\bar{u} \rightarrow u\bar{u}) + \frac{d\sigma}{dt}(u\bar{u} \rightarrow \bar{u}u) + \frac{d\sigma}{dt}(u\bar{u} \rightarrow d\bar{d}) + \frac{d\sigma}{dt}(u\bar{u} \rightarrow \bar{d}d) - \frac{d\sigma}{dt}(uu \rightarrow uu) \right]. \quad (3.5)$$

Combining the lowest-order expressions for the different cross sections¹⁰ gives

$$\frac{d\sigma^{\text{ah}}}{dt}(s, t, u) = 2 \frac{\pi\alpha_s^2}{s} \left[-\frac{16}{9} \left[\frac{t^2 + u^2}{s^2} \right] + \frac{8}{27} \left[\frac{s^3 + t^3 + u^3}{stu} \right] \right]. \quad (3.6)$$

In addition, we must consider the annihilation of quarks into final-state gluons:

$$\frac{d\sigma^{u\bar{u} \rightarrow GG}}{dt}(s, t, u) = 2 \frac{\pi\alpha_s^2}{s} \left[-\frac{8}{3} \left[\frac{t^2 + u^2}{s^2} \right] + \frac{32}{27} \left[\frac{t^2 + u^2}{ut} \right] \right]. \quad (3.7)$$

After the subtractions, therefore, we can write the nonsinglet spin-averaged observable (3.1) in the form

$$\begin{aligned} \frac{E d\sigma^{\text{DV}}}{d^3p}(\pi^0) &= \frac{1}{\pi} \int dx_a dx_b [u_v(x_a, \mu^2)u_v(x_b, \mu^2) + d_v(x_a, \mu^2)d_v(x_b, \mu^2)] \\ &\times \left[\frac{1}{z_c} D_{\pi^0/q}(z_c) \frac{d\sigma^{\text{ah}}}{d\hat{t}}(\hat{s}, \hat{t}, \hat{u}) + \frac{1}{z_c} D_{\pi^0/G}(z_c) \frac{d\sigma^{u\bar{u} \rightarrow GG}}{d\hat{t}}(\hat{s}, \hat{t}, \hat{u}) \right] [1 + O(\alpha_s/\pi)], \end{aligned} \quad (3.8)$$

which depends only on the valence-quark distributions $u_v(x, \mu^2)$ and $d_v(x, \mu^2)$. In order to isolate a spin-dependent valence observable we can start with

$$a_{LL} \frac{E d\sigma}{d^3p}(pp \rightarrow \pi^0 x) \equiv \frac{1}{\pi} \sum_{ab \rightarrow cd} \int dx_a dx_b \Delta G_{a/p}(x_a, \mu^2) \Delta G_{b/p}(x_b, \mu^2) \frac{1}{z_c} D_{\pi^0/c}(z_c, \mu^2) \left[a_{LL} \frac{d\sigma}{dt}(ab \rightarrow cd) \right] \quad (3.9)$$

as in the spin-averaged case. Taking the difference between $p\bar{p}$ and pp initial states picks out the ‘‘annihilation’’ spin asymmetry at the quark level,

$$\begin{aligned}
a_{LL} \frac{d\sigma^{\text{ah}}}{dt}(s,t) &= \left[a_{LL} \frac{d\sigma}{dt}(u\bar{u} \rightarrow u\bar{u}) + a_{LL} \frac{d\sigma}{dt}(u\bar{u} \rightarrow \bar{u}u) + a_{LL} \frac{d\sigma}{dt}(u\bar{u} \rightarrow \bar{d}d) \right. \\
&\quad \left. + a_{LL} \frac{d\sigma}{dt}(u\bar{u} \rightarrow d\bar{d}) - a_{LL} \frac{d\sigma}{dt}(uu \rightarrow uu) \right] \\
&= 2 \frac{\pi\alpha_s^2}{s} \left[-\frac{16}{9} \frac{t^2+u^2}{s^2} + \frac{8}{27} \frac{s^3+t^3+u^3}{stu} \right], \tag{3.10}
\end{aligned}$$

which vanishes at $\theta_{\text{c.m.}} = 90^\circ$. The spin asymmetry for the annihilation of $q\bar{q}$ into gluons is

$$a_{LL} \frac{d\sigma^{u\bar{u} \rightarrow GG}}{dt}(s,t,u) = -\frac{2\pi\alpha_s^2}{s} \left[-\frac{8}{3} \left[\frac{t^2+u^2}{s^2} \right] + \frac{32}{27} \left[\frac{t^2+u^2}{ut} \right] \right] \tag{3.11}$$

corresponding to annihilation taking place only in the $+-$ helicity configuration. Taking the difference between $p\bar{p}$ and pp collisions then gives the expression

$$\begin{aligned}
a_{LL} \frac{E d\sigma}{d^3p}(p\bar{p} \rightarrow \pi^0 x) - a_{LL} \frac{E d\sigma}{d^3p}(pp \rightarrow \pi^0 x) &= \frac{1}{\pi} \int dx_a dx_b [\Delta u_{\text{val}}(x_a, \mu^2) \Delta u_{\text{val}}(x_b, \mu^2) + \Delta d_{\text{val}}(x_a, \mu^2) \Delta d_{\text{val}}(x_b, \mu^2)] \\
&\quad \times \left[\frac{1}{z_c} D_{\pi^0/u}(z_c) a_{LL} \frac{d\sigma^{\text{ah}}}{d\hat{t}}(\hat{s}, \hat{t}, \hat{u}) \right. \\
&\quad \left. + \frac{1}{z_c} D_{\pi^0/G}(z_c) a_{LL} \frac{d\sigma^{u\bar{u} \rightarrow GG}}{d\hat{t}}(\hat{s}, \hat{t}, \hat{u}) \right] \left[1 + O\left[\frac{\alpha_s}{\pi}\right] \right]. \tag{3.12}
\end{aligned}$$

Taking the ratio of (3.12) and (3.8) we get

$$A_{LL}^{\text{DV}}(\pi^0) = \frac{a_{LL} d\sigma(p\bar{p} \rightarrow \pi^0 x) - a_{LL} d\sigma(pp \rightarrow \pi^0 x)}{d\sigma(p\bar{p} \rightarrow \pi^0 x) - d\sigma(pp \rightarrow \pi^0 x)} \tag{3.13}$$

entirely in terms of valence quantities. Figure 3 shows the estimate for this ratio using the distribution functions given in Sec. II. As mentioned there, because of the method used in determining the distribution $\Delta u_{\text{val}}(x, \mu^2)$ from the models in Ref. 14, there is some dependence on the assumptions concerning the polarization of sea quarks. This ambiguity is indicated by the difference in the two curves in the figure.

The same arguments can be repeated for other processes including the production of direct photons. We will not go into the procedure in detail because the basic form can be deduced rather easily. Taking the difference between $p\bar{p} \rightarrow \gamma X$ and $pp \rightarrow \gamma X$ cancels the contribution of the $qG \rightarrow \gamma q$ and $\bar{q}G \rightarrow \gamma \bar{q}$ subprocess. This isolates the $q\bar{q} \rightarrow \gamma G$ annihilation subprocess, with the cross section

$$\frac{d\sigma^{q\bar{q} \rightarrow \gamma G}}{d\hat{t}} = \frac{\pi\alpha\alpha_s}{s^2} \frac{8}{9} \left[\frac{\hat{t}^2 + \hat{u}^2}{\hat{u}\hat{t}} \right]. \tag{3.14}$$

Helicity conservation gives the spin-weighted cross section

$$a_{LL} \frac{d\sigma^{q\bar{q} \rightarrow \gamma G}}{d\hat{t}} = - \left[\frac{d\sigma}{d\hat{t}} \right]^{q\bar{q} \rightarrow \gamma G} \tag{3.15}$$

and we have the difference between $p\bar{p} \rightarrow \gamma X$ and $pp \rightarrow \gamma X$ in the form

$$\frac{E d\sigma^{\text{DV}}}{d^3p}(\gamma) = \frac{1}{\pi} \int_{x_{\text{min}}}^1 dx_a \left[\frac{x_a x_b}{x_a - x_T} \right] \left[\frac{4}{9} u_v(x, \mu^2) u_v(x, \mu^2) + \frac{1}{9} d_v(x, \mu^2) d_v(x, \mu^2) \right] \left[\frac{d\sigma^{q\bar{q} \rightarrow \gamma G}}{d\hat{t}}(\hat{s}, \hat{t}, \hat{u}) \right], \tag{3.16}$$

where we have pulled the quark charge factors into the distribution. With a similar expression for the spin-weighted difference we can take the ratio to produce the curves in Fig. 4. Again, the separate curves show the residual dependence on polarized sea distributions.

The experimental determination of the asymmetries $A_{LL}^{\text{DV}}(\pi^0)$ and $A_{LL}^{\text{DV}}(\gamma)$ requires a polarized proton target as well as polarized beams of both protons and antipro-

tons. It is obviously a nontrivial experimental challenge to assemble these elements in a single experiment, to control the systematics, and to collect meaningful data. The payoff seems purely theoretical in that, using the usual factorization properties, the observable can be compared with a QCD-based hard-scattering calculation involving only valence-quark distributions. Effects associated with the unmeasured gluon polarization and with the poorly

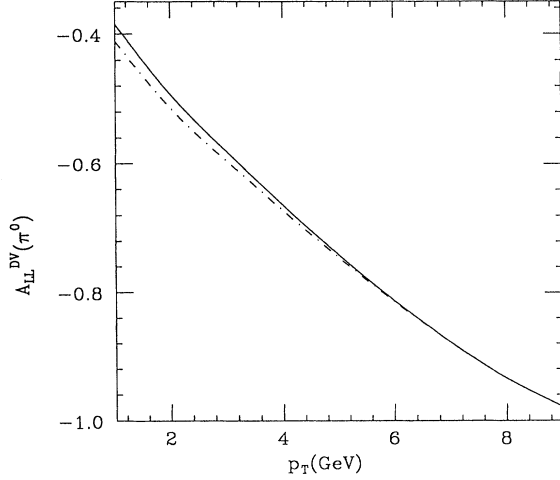


FIG. 3. A prediction for the asymmetry $A_{LL}^{DV}(\pi^0)$ representing the difference between the $(p\bar{p})$ and (pp) asymmetries for pion production, as a function of p_T . The distinction between curves is an indication of the difference of interpretations in the valence-quark distribution as discussed in Sec. II of the text. Figures 3 and 4 are shown at $\sqrt{s} = 20$ GeV.

determined polarization of the sea quarks are canceled in the difference. In the framework of QCD, the lack of agreement between the measurement can therefore be attributed either to higher-twist effects or to the presence of very large higher-order terms in the perturbative expansion.

In fact, the chiral properties of QCD provide considerable aid in estimating the size of higher-order perturbative corrections to two-spin asymmetries. They turn out to be better controlled than the higher-order corrections to spin-averaged cross sections. This is important since, in general the higher-order corrections to the inclusive

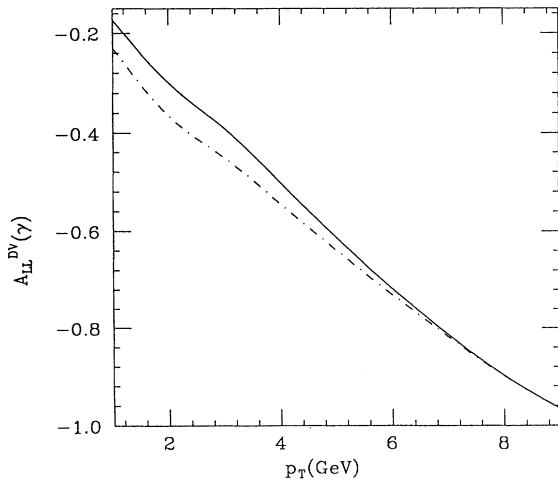


FIG. 4. The asymmetry $A_{LL}^{DV}(\gamma)$ for direct photon production, representing a similar difference as that shown in Fig. 3.

production of high- p_T hadrons have been found to be large. Of course, the size of the corrections depends on the factorization and renormalization prescription employed in the calculation.²⁸ However, a short exercise can show the main advantage of calculating a spin asymmetry. If we write the next-to-leading-order calculation for a process such as $qq \rightarrow qX$ in the form

$$\begin{aligned} d\hat{\sigma}(++) &= d\sigma_{++}^{(o)} \left[1 + \frac{\alpha_s}{\pi} K + \frac{\alpha_s}{\pi} \delta K + \dots \right], \\ d\hat{\sigma}(+-) &= d\sigma_{+-}^{(o)} \left[1 + \frac{\alpha_s}{\pi} K - \frac{\alpha_s}{\pi} \delta K + \dots \right], \end{aligned} \quad (3.17)$$

examination of the appropriate diagrams²⁹ shows that the major part of the correction is independent of the initial quark spins. For a convenient choice of prescriptions, we have therefore

$$\delta K \ll K. \quad (3.18)$$

Then, the spin asymmetry is given by

$$\begin{aligned} A &= \frac{d\hat{\sigma}(++) - d\hat{\sigma}(+-)}{d\hat{\sigma}(++) + d\hat{\sigma}(+-)} \\ &\cong A^{(o)} + [1 - (A^{(o)})^2 + \dots] \frac{\alpha_s}{\pi} \delta K', \end{aligned} \quad (3.19)$$

where $A^{(o)}$ is the lowest-order asymmetry and

$$\delta K' = \frac{\delta K}{1 + (\alpha_s/\pi)K}. \quad (3.20)$$

This means that if we choose a set of conventions with K large so that $(\alpha_s/\pi)K$ cannot be ignored in the calculation of the spin-averaged cross section, we still have reason to take seriously the Born term estimate for the two-spin asymmetry. For a valence quantity such as $A_{LL}^{DV}(\pi^0)$, if we stay away from the edges of phase space, the theoretical uncertainties in the hard-scattering calculation are commensurate with the errors associated with the specification of the parton distributions.

Of course, at a given p_T and s , coherent effects or higher-twist corrections may make the comparison between theory and experiment unreliable. The hope is that we can go to a kinematic region where these effects are small. If they are small for A_{LL}^{DV} , there arises the additional hope that they are small for the individual asymmetries separately. We can then look at measurements of $a_{LL} d\sigma(pp \rightarrow \pi^0 X)$ or $a_{LL} d\sigma(pp \rightarrow \gamma X)$ at these values of p_T as ‘‘measurements’’ of the spin-weighted gluon distribution.

IV. SENSITIVITY TO THE POLARIZED GLUON DISTRIBUTION FOR TWO-SPIN ASYMMETRIES

The valence-dominated processes discussed in Sec. III allow one to sidestep the unknown contributions from polarized gluons and to focus directly on the question of the overall validity of the hard-scattering QCD model for spin-weighted observables. In the absence of such experimental cross-checks, an effect observed in $A_{LL}(pp \rightarrow \pi^0 X)$ which should be associated with subasymptotic, higher-

twist connections, might erroneously be attributed to polarized gluons. However, as mentioned above, interest in the spin structure of the nucleon compels an experimental program with the goal of "measuring" gluon polarization.

It would be convenient if it were possible to experimentally isolate polarized gluons in a number of different processes. The production of direct photons provides the best opportunity to do this in that one can find a kinematic region where the subprocess $qG \rightarrow q\gamma$ is dominant. Hidaka¹¹ first emphasized the advantages of measuring the gluon polarization by means of $A_{LL} d\sigma(pp \rightarrow \gamma X)$ and this has been reiterated by a number of authors.^{4,14,27} An

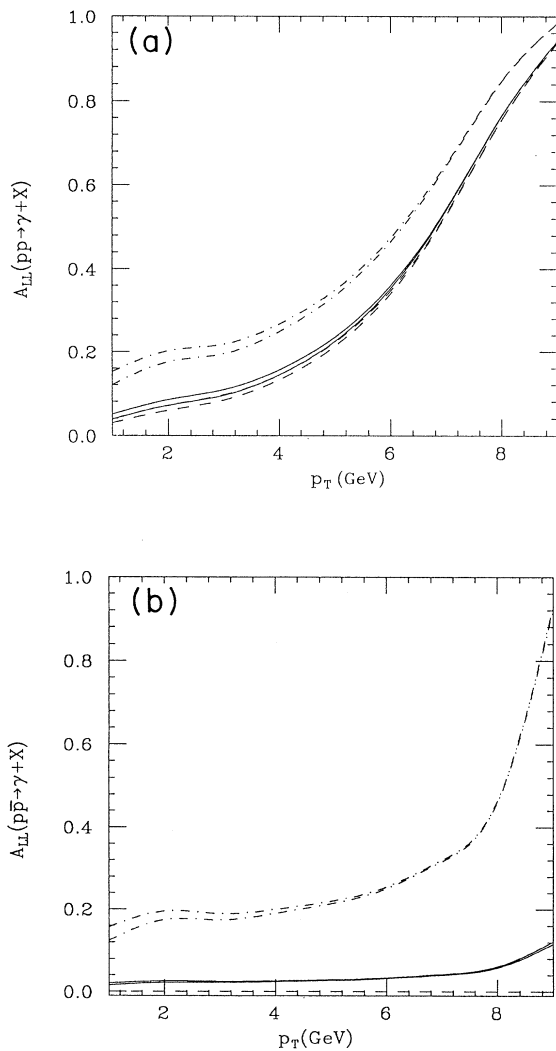


FIG. 5. The asymmetries for direct photon production at $\sqrt{s} = 20$ GeV. (a) shows the asymmetry for pp scattering, while (b) illustrates the asymmetry for $p\bar{p}$ scattering. The dot-dashed curves are the asymmetries for the large gluon polarization, given two different models for the polarized sea distribution. The solid curves similarly represent the asymmetry with the small gluon polarization and the dashed lines with no gluon polarization.

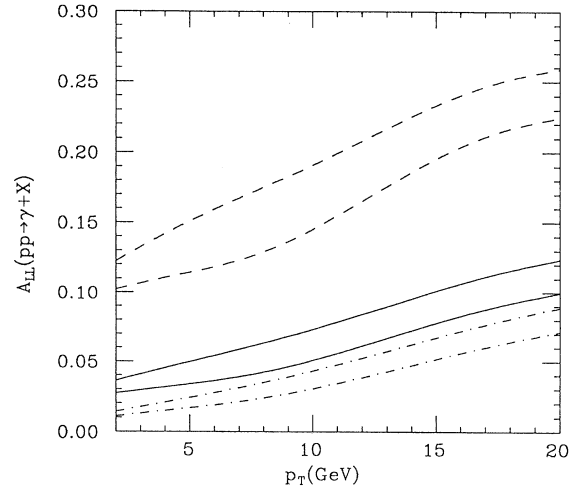


FIG. 6. The direct photon asymmetries at $\sqrt{s} = 200$ GeV, an energy possibly attainable at RHIC. Dashed curves correspond to the large gluon polarization, the solid curves represent the small gluon polarization and the dot-dashed curves no gluon polarization.

additional bonus for direct photon production is that the next-to-leading-order calculation has been done for the spin-averaged cross section. Examination of the dominant corrections confirms that they are independent of the initial spin configurations so that the condition (3.18) should be met. There is, of course, the problem that because direct photon production is electromagnetic, the cross section is small and is difficult to get to large values of p_T . At values of p_T accessible in fixed-target experiments it will be difficult to separate higher-twist effects. Measurement of $A_{LL}^{DY}(\gamma)$ as advocated in Sec. III will provide some handle on the problem. The possibility of polarized beams injected into pp colliders such as the

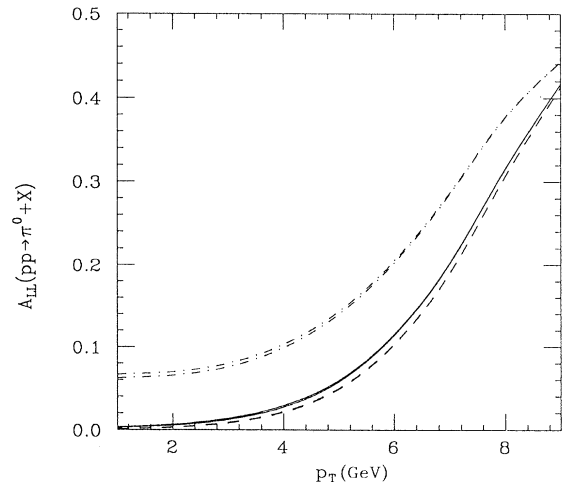


FIG. 7. The asymmetries for pion production ($pp \rightarrow \pi^0 + X$) at $\sqrt{s} = 20$ GeV. The curves represent the same gluon models as those in Fig. 5.

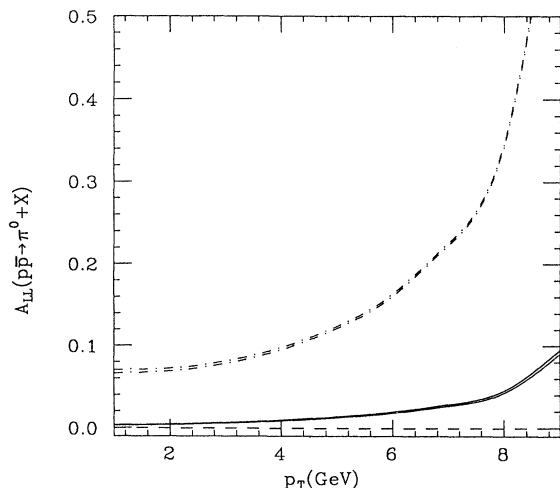


FIG. 8. The same asymmetries as in Fig. 7 shown for $(p\bar{p} \rightarrow \pi^0 + X)$ at $\sqrt{s} = 20$ GeV.

BNL Relativistic Heavy Ion Collider³⁰ (RHIC) should allow an opportunity to measure this asymmetry at large values of p_T where subasymptotic corrections can be negligible. In Figs. 5(a) and 5(b) we show plots of $A_{LL}(p\bar{p} \rightarrow \gamma X)$ and $A_{LL}(pp \rightarrow \gamma X)$ for the three different models of the gluon polarization discussed in Sec. II. Note that it is difficult to discriminate between the case of weak gluon polarization and no gluon polarization.

Figure 6 shows $A_{LL}(pp \rightarrow \gamma X)$ for $\sqrt{s} = 200$ GeV (an energy which might be accessible at RHIC). At this energy, the asymmetries are small, but well separated by the various gluon models.

The individual measurements $A_{LL}(pp \rightarrow \pi^0 X)$ and $A_{LL}(p\bar{p} \rightarrow \pi^0 X)$ should also be sensitive to the gluon polarization density. For these processes the contribution

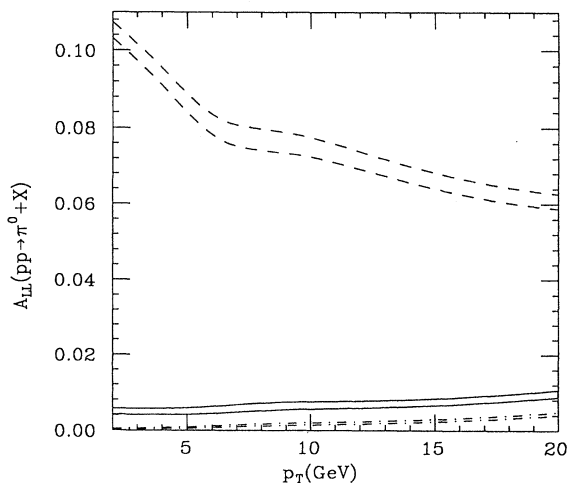


FIG. 9. The asymmetries for $(pp \rightarrow \pi^0 + X)$ at $\sqrt{s} = 200$ GeV. The curves represent the same polarized gluon models as those in Fig. 6.

from the valence-quark processes can be reliably estimated provided that there are no incalculable higher-twist effects. In Fig. 7 we show our calculation for $A_{LL}(pp \rightarrow \pi^0 X)$ at $\sqrt{s} = 20$ GeV for the three different gluon distributions. Figure 8 shows the same curves for $A_{LL}(p\bar{p} \rightarrow \pi^0 X)$. There is good discrimination between the curves for strong gluon polarization and the other two possibilities. However, given the theoretical error associated with the quark polarizations, it would be very difficult to measure $A_{LL}(pp \rightarrow \pi^0 X)$ with the accuracy necessary to discriminate the “weak polarization” and the “no-polarization” models for the gluon spin density.

Figure 9 shows the calculation for $A_{LL}(pp \rightarrow \pi^0 X)$ at $\sqrt{s} = 200$ GeV. The Q^2 evolution of the parton distributions provides the difference between this graph and Fig.

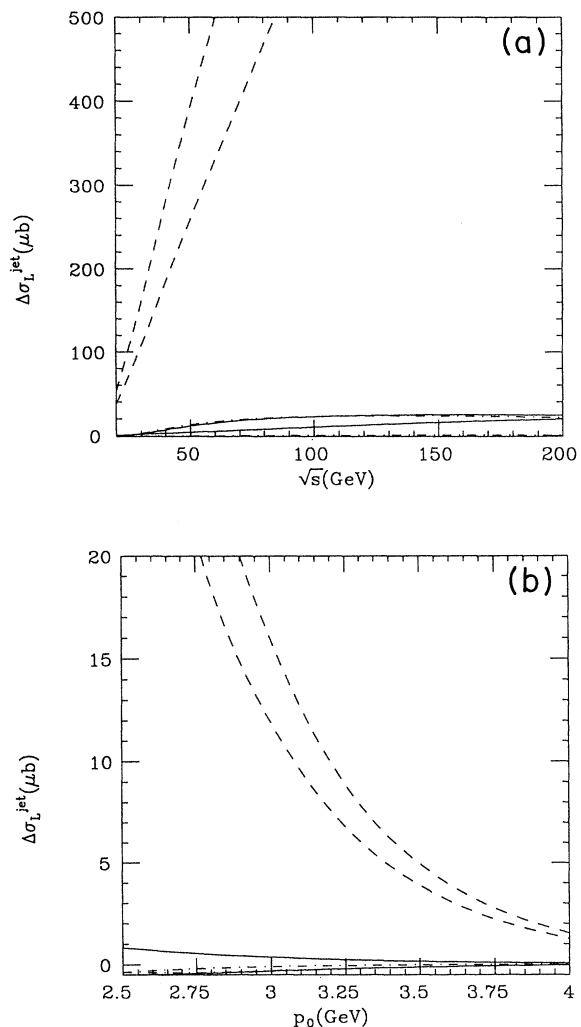


FIG. 10. (a) The polarized jet cross section $\Delta\sigma_L^{\text{jet}}$ as a function of \sqrt{s} for a momentum cutoff for distinguishing a jet, $p_0 = 2.5$ GeV; (b) the same jet cross section as a function of p_0 at $\sqrt{s} = 20$. Solid curves, small ΔG ; dashed curves, large ΔG ; dot-dashed curve, $\Delta G = 0$. All are plotted with the two polarized sea models mentioned in the text.

7. From these figures we see that both direct photon production and π^0 production have the feature that the longitudinal spin-spin asymmetry can support or rule out the idea of very strong polarization of the gluons in a polarized proton. In order to distinguish gluon-originated asymmetries from higher-twist effects, measurements of $A_{LL}^{DV}(\pi^0)$ or $A_{LL}^{DV}(\gamma)$ can provide a crucial calibration of the underlying theoretical framework.

It remains an open challenge to design an experiment with the precision necessary to distinguish the possibilities

$$\left. \frac{\Delta G(x, \mu^2)}{G(x, \mu^2)} \right|_{\mu^2=10 \text{ GeV}^2} \cong x, \quad \left. \frac{\Delta G(x, \mu^2)}{G(x, \mu^2)} \right|_{\mu^2=10 \text{ GeV}^2} \cong 0$$

which define a reasonable range of ‘‘conventional’’ dynamical mechanisms for gluon polarization. To do this, both control of valence quantities (using measurements of A_{LL}^{DV}) and high luminosity seem to be necessary. Polarized beams in future storage rings (such as RHIC,

the CERN Large Hadron Collider, or the Superconducting Super Collider) provide the potential for such measurements.

As a final quantity which can provide an estimate of the gluon polarization, we consider $\Delta\sigma_L^{\text{jet}}(pp; p_0, \sqrt{s})$. This cross section was discussed in Ref. 17. In Ref. 18 we pointed out that it could provide an early signal for a large $\Delta G(x, Q^2)$. Since this type of observable is particularly well suited for experiments in colliding beams, we give in Fig. 10 a set of plots of $\Delta\sigma_L^{\text{jet}}$ as a function of \sqrt{s} at fixed p_0 and $\Delta\sigma_L^{\text{jet}}$ as a function of p_0 at fixed \sqrt{s} , for our three models of the gluon distribution. These curves can give a feel for the type of experimental precision needed in future experiments.

ACKNOWLEDGMENTS

We would like to thank the members of the Fermilab experiment E-704 for testing their data with the suggestions in this paper. This work was supported by the U.S. Department of Energy, Division of High Energy Physics, Contract No. W-31-109-ENG-38.

¹European Muon Collaboration, J. Asham *et al.*, Phys. Lett. B **206**, 309 (1988).

²J. Ellis and R. L. Jaffe, Phys. Lett. B **193**, 101 (1987).

³F. Close and R. G. Roberts, Phys. Rev. Lett. **60**, 1471 (1988).

⁴S. Brodsky, J. Ellis, and M. Karliner, Phys. Lett. B **206**, 309 (1988).

⁵M. Anselmino, B. Iogge, and E. Leader, Yad. Fiz. **49**, 214 (1989) [Sov. J. Nucl. Phys. **49**, 136 (1989)].

⁶J. Ellis and M. Karliner, Phys. Lett. B **213**, 73 (1988).

⁷G. Preparata and J. Soffer, Phys. Rev. Lett. **61**, 1167 (1988).

⁸H. Lipkin, Phys. Lett. B **214**, 429 (1988); **230**, 135 (1989).

⁹J. D. Bjorken, Phys. Rev. **148**, 467 (1966).

¹⁰J. Babcock *et al.*, Phys. Rev. Lett. **40**, 1161 (1978); Phys. Rev. D **19**, 1483 (1979).

¹¹K. Hidaka, Phys. Rev. D **21**, 1316 (1980); Nucl. Phys. **B192**, 369 (1981); N. Craigie, K. Hidaka, M. Jacob, A. Penzo, and J. Soffer, *ibid.* **B204**, 365 (1982).

¹²For a discussion of corrections in high- p_T processes, see, e.g., A. P. Contogouris and H. Tonaka, Phys. Rev. D **33**, 1265 (1986).

¹³R. Roberts and J. Sterling, report, 1990 (unpublished).

¹⁴J. Qiu, G. Ramsey, D. Richards, and D. Sivers, Phys. Rev. D **41**, 65 (1990).

¹⁵G. Altarelli and G. G. Ross, Phys. Lett. B **212**, 391 (1988).

¹⁶R. D. Carlitz, J. Collins, and A. H. Mueller, Phys. Lett. B **214**,

229 (1989).

¹⁷G. P. Ramsey, D. Richards, and D. Sivers, Phys. Rev. D **37**, 314 (1988).

¹⁸G. P. Ramsey and D. Sivers, Report No. ANL-HEP-PR-89-89 (unpublished).

¹⁹G. Bodwin, Phys. Rev. D **31**, 2616 (1985); **34**, 3932 (1986); J. C. Collins, D. E. Soper, and G. Sterman, Nucl. Phys. **B261**, 104 (1985); **B308**, 833 (1988).

²⁰R. C. Carlitz and J. Kaur, Phys. Rev. Lett. **38**, 673 (1977); J. Kaur, Nucl. Phys. **B128**, 219 (1977).

²¹See, for example, J. Mandula, J. Govaerts, and G. Zweig, Nucl. Phys. **B228**, 109 (1983).

²²G. Altarelli and G. Parisi, Nucl. Phys. **B126**, 298 (1977).

²³P. Ratcliff, Phys. Lett. B **192**, 180 (1987).

²⁴M. Einhorn and J. Soffer, Nucl. Phys. **B274**, 714 (1986).

²⁵G. Bodwin and J. Qiu, Phys. Rev. D **41**, 2755 (1990).

²⁶R. Jaffe and A. Manohar, MIT report (unpublished).

²⁷E. Berger and J. Qiu, Phys. Rev. D **40**, 778 (1989).

²⁸W. Celmaster and D. Sivers, Ann. Phys. (N.Y.) **143**, 1 (1982).

²⁹P. Aurenche *et al.*, Phys. Lett. **140B**, 87 (1984).

³⁰Polarized beams at RHIC are a possibility under consideration. For further information see the Proceedings of the Polarized Collider Workshop, University Park, Pennsylvania, 1990 (unpublished).